Available online at www.sciencedirect.com
SCIENCE DIRECT®
Journal of Solid State Chemistry 178 (2005) 3571–3580
JOURNAL OF SOLID STATE CHEMISTRY
www.elsevier.com/locate/jssc

Acid and redox properties of mixed oxides prepared by calcination of chromate-containing layered double hydroxides

M. del Arco, D. Carriazo, C. Martín, A.M. Pérez-Grueso, V. Rives*

Dpto. Química Inorgánica, Universidad de Salamanca, 37008-Salamanca, Spain

Received 27 July 2005; received in revised form 6 September 2005; accepted 11 September 2005
Available online 11 October 2005

Abstract

Layered double hydroxides (LDHs) with Mg and Al in the layers and carbonate, nitrate or chloride in the interlayer, or with Zn and Al in the layers and chloride in the interlayer, have been prepared by coprecipitation, and have been used as precursors to prepare chromate-containing LDHs. All these systems, as well as those obtained upon their calcination up to 800 °C, have been characterised by powder X-ray diffraction, FT-IR and vis–UV spectroscopies, temperature-programmed reduction (TPR), nitrogen adsorption at −196 °C for surface texture and porosity assessment, and FT-IR monitoring of pyridine adsorption for surface acidity determination. The results obtained show that the crystallinity of the chromate-containing LDH depends on the precursor used. The layered structure of the Mg, Al systems is stabilised up to 400 °C upon incorporation of chromate; however, the Zn,Al-chromate samples collapse between 200 and 300 °C, with simultaneous formation of ZnO. Calcination of the samples above 400 °C gives rise to a reduction of Cr(VI) to Cr(III), as concluded from vis–UV spectroscopic studies. The TPR profiles show that chromate in ZnAl hydrotalcite is more easily reduced than that incorporated in the magnesium ones. Moderately strong surface Lewis acid sites exist in all samples calcined below 500 °C.

Keywords: Chromate intercalated; Hydrotalcite; Acid properties

1. Introduction

Several hydroxides of divalent cations exhibit the structure of brucite—$Mg(OH)_2$-forming layers constituted by edge-sharing octahedra [1,2]. If the ionic radii of the cations are between ca. 0.6 and 0.7 Å, they can be easily substituted (up to a certain substitution degree) by trivalent cations. This substitution gives rise to solids whose chemical formula can be written as $[M_{1-x}^{2+}M_x^{3+}(OH)_2]^{x+}$, where an excess of positive charge exists, which is balanced by anions located between the brucite-like layers, together with water molecules. In this way, a large variety of solids with different layer anions and different layer cations have been prepared, in addition to those solids existing in nature also showing this structure. These solids are usually known as layered double hydroxides (LDHs), hydrotalcites—because of the natural compound hydrotalcite, $Mg_6Al_2(OH)_8CO_3 \cdot 2H_2O$—or also anionic clays [3–10]. The interest in these materials has shown an outstanding growth in recent years due to their varied applications as catalysts or catalyst precursors, adsorbents—their exchange capacity can be as large as 3 meq/g—sensors, fillers, drug support, etc. These solids are obtained by direct synthesis (coprecipitation from solutions of the metal cations in a solution of the anion to be intercalated), or by reconstruction of precursor LDHs calcined at moderate temperatures, or by ion exchange of the interlayer anion; obviously, not all the methods can be used for a given material.

Intercalation of bulk anions containing metal anions in a high oxidation state (e.g., oxometalates such as decavanadate, molybdate, or chromate) modifies their catalytic properties, due to developing of acid and red–ox sites and, in some cases, interlayer microporosity. Eventually they can even increase the thermal stability acting as real pillars between the layers.

Several papers have been published so far on LDHs containing intercalated chromate; very few of them have dealt with their physicochemical properties [11–14], and

*Corresponding author. Fax: +34 923 29 45 74.
E-mail address: vrives@usal.es (V. Rives).

0022-4596/$ - see front matter © 2005 Elsevier Inc. All rights reserved.
doi:10.1016/j.jssc.2005.09.014

many studies have been devoted to analyse the use of these materials for scavenging chromate anions from water solutions [15–19]. Here we report a study on the preparation of MgAl–CrO_4 and ZnAl–CrO_4 systems. These samples, as well as the solids obtained by calcination, have been characterised by powder X-ray diffraction (PXRD), Fourier transform infrared (FT-IR) and vis–UV spectroscopies, temperature-programmed reduction (TPR) and pyridine adsorption, monitored by FT-IR spectroscopy. Our main interest was to evaluate the nature of the species present in the different systems and to monitor the evolution of their structural and properties as a function of the calcination temperature.

2. Experimental

2.1. Preparation of the samples

The MgAl–CrO_4 LDHs have been prepared by reconstruction or anion exchange using MgAl-CO_3 or MgAl-NO_3 LDHs (for reconstruction) and MgAl-Cl for anion exchange. The ZnAl–CrO_4 system—for which a larger surface acidity is expected—has been prepared by anion exchange from a ZnAl-Cl hydrotalcite. The molar M^{2+}/M^{3+} ratio in the starting solutions was always 2.0. All reagents were from Panreac and were used as purchased, without any further purification, except gases, which had been supplied by L'Air Liquide (Spain).

The MgAl-CO_3 sample (hereafter MgAlC) was prepared by coprecipitation from aqueous solutions of $Mg(NO_3)_2 \cdot 6H_2O$ and $Al(NO_3)_3 \cdot 9H_2O$ following the method described by Reichle [20]. Sample MgAl-NO_3 (hereafter MgAlN) was prepared by coprecipitation at pH = 9 following the method described elsewhere [21]. Samples MgAl-Cl and ZnAl-Cl (hereafter MgAlCl and ZnAlCl, respectively) were prepared by coprecipitation in a N_2 atmosphere (to avoid incorporation of carbonate from atmospheric carbon dioxide) from aqueous solutions of $MgCl_2 \cdot 6H_2O$ (or $ZnCl_2$) and $AlCl_3 \cdot 6H_2O$ at pH = 9 (sample MgAlCl) or 8 (sample ZnAlCl), using 2 M NaOH; the precise experimental conditions to prepare each sample were carefully chosen after several trials. The suspensions were aged for 24 h at room temperature (r.t.) without stirring or at 70 °C and simultaneous stirring for samples ZnAlCl and MgAlCl, respectively. The precipitates were left in suspension under a nitrogen atmosphere until they were used for anion exchange.

Incorporation of chromate was carried out following two routes, reconstruction and anion exchange. To prepare the samples by *reconstruction*, 2 g of the MgAlC or MgAlN precursor was calcined in a tubular furnace up to 500 °C under a nitrogen flow at a heating rate of 5 °C min^{-1}, the final temperature being maintained for 3 h. The solid was added to an aqueous solution of potassium chromate. The pH of the suspension was adjusted to 9 for the MgAlC precursor using 2 M HNO_3 (higher pH values did not give rise to chromate insertion in the interlayer), although for the MgAlN precursor the pH was left to the unmodified value of the solution (11.5). The suspensions so far obtained were stirred under inert atmosphere (N_2) at r.t. for 12 h (MgAlC) or 6 h (MgAlN). The solids were then filtered, washed with decarbonated water and dried in a vacuum desiccator; these samples, prepared from precursors MgAlC and MgAlN, are named MgCCr and MgNCr, respectively.

A second set of samples was prepared by *anion exchange* following a method similar to that described by Roy et al. [22]. The suspensions of LDH precursors MgAlCl and ZnAlCl were maintained at the original pH values of 9 and 8.5, respectively, which were mixed with the same chromate solution used to prepare the samples by reconstruction. The suspensions were magnetically stirred at r.t. for 24 h under a nitrogen atmosphere (to avoid carbonation by atmospheric CO_2), and then were washed with decarbonated water, centrifuged and dried in a vacuum desiccator, yielding samples MgClCr and ZnClCr, respectively, when starting from precursors MgAlCl and ZnAlCl.

In all cases, the amount of chromate was twice that necessary to balance the positive charge of the layers, due to the M^{2+}/Al^{3+} substitution, i.e., a CrO_4^{2-}/Al^{3+} molar ratio of 1. To study the phases formed upon thermal decomposition, the samples were calcined at temperatures ranging from 100 to 800 °C at 5 °C/min with a dwell time of 6 h.

2.2. Characterisation procedures

Element chemical analyses for Mg, Al, Zn, and Cr were carried out in Servicio General de Análisis Químico Aplicado (University of Salamanca, Spain) by atomic absorption in a Mark-2 EEL 240 apparatus, after dissolving the samples in nitric acid. The carbon content was determined in a CHNS 932 Leco analyser and chlorine was determined following the Volhard method [23]. The PXRD patterns were obtained by reflection from powder packed in a sample holder, with a Siemens D-500 diffractometer, using Cu $K\alpha$ radiation ($\lambda = 1.54050$ Å) with a graphite monochromator and interfaced to a DACO-MP data acquisition microprocessor. FT-IR spectra were collected in a Perkin Elmer FT-1730 instrument using de KBr pellet technique; 100 scans were averaged to improve the signal-to-noise ratio, at a nominal resolution of 4 cm^{-1}. The UV–vis spectra of the samples were recorded following the diffuse reflectance technique (UV–vis/DR) in a PERKIN ELMER LAMBDA 35 instrument equipped with a Labsphere RSA-PE-20 and connected to a PC with UV WINLAB 2.85 software. The nitrogen adsorption–desorption isotherms for specific surface area and porosity assessment were recorded at −196 °C in a Gemini instrument from Micromeritics. TPR analyses were carried out on the unpretreated samples in a Micromeritics TPR/TPD 2900 instrument, at a heating rate of 10 °C min^{-1}, using ca. 15 mg of samples and 60 mL/min of a H_2/Ar mixture (5 vol%) as reducing agent; these

experimental conditions were chosen to obtain good resolution of the reduction peaks [24].

Surface acidity monitoring was carried out by FT-IR spectroscopic study of pyridine adsorption in a Perkin-Elmer 16 PC spectrometer coupled to a high-vacuum Pyrex system and using self-supported discs, degassed in situ in a special cell [25] built in Pyrex, but with CaF_2 windows (transparent to the IR radiation in the required wavenumbers range) at 400 °C for 2 h, prior to pyridine adsorption. The spectrometer is coupled to a PC, and commercial software was use to process the spectra. Fifty scans were recorded to improve the signal-to-noise ratio, at a nominal resolution of 2 cm^{-1}. The gas is admitted to the IR-adsorption cell at r.t., and after 15 min for equilibration, the gas phase is removed by outgassing at different temperatures (r.t.−400 °C) and the spectrum is recorded.

3. Results and discussion

From element chemical analysis the following formulae have been calculated for the precursor samples: $[Mg_{0.63}Al_{0.36}(OH)_2](CO_3)_{0.18}\cdot nH_2O$, $[Mg_{0.67}Al_{0.33}(OH)_2](NO_3)_{0.33}\cdot nH_2O$, $[Mg_{0.67}Al_{0.33}(OH)_2](Cl)_{0.30}(CO_3)_{0.02}\cdot nH_2O$ and $[Zn_{0.61}Al_{0.39}(OH)_2](Cl)_{0.33}(CO_3)_{0.03}\cdot nH_2O$ for samples MgAlC, MgAlN, MgAlCl and ZnAlCl, respectively. The M^{2+}/Al^{3+} molar ratios are similar to those existing in the starting solutions, except for sample ZnAlCl, for which the Zn/Al molar ratio is as low as 1.6. The chloride-LDHs are partially carbonated, despite the careful conditions used during synthesis.

The element chemical analyses for the chromate-containing LDHs are given in Table 1, together with the formulae calculated for these samples. The largest chromate loading is achieved when starting from sample MgAlCl, although in all samples, a small portion of carbonate still seems to be present.

The PXRD diagrams for the precursors and for the chromate-LDHs are included in Fig. 1. The lattice parameters a and c, calculated assuming [26] a $R3M$ symmetry are also included in Table 1. All the diagrams recorded are consistent with the presence of well crystallised hydrotalcite-like compounds, showing the three characteristic basal reflections due to planes (003), (006), and (009). The diffraction peaks in the diagrams of the precursors are very sharp and intense, while those for the chromate-containing samples are broader and less intense, especially for sample MgCCr, suggesting a low crystallinity and a less organised stacking arrangement [27].

The change in basal spacing (from the position of the first intense maximum at low 2θ values) indicates that chromate has been actually intercalated in all cases. The spacing for the first peak, ascribed to diffraction by planes (003), ranges from 8 to 8.6 Å. If the width of the brucite-like layer (4.8 Å [28]) is subtracted, the gallery height results 3.2–3.8 Å, slightly lower than the size of the tetrahedral anion CrO_4^{2-}, with a thermochemical radius of 2.4 Å [29]; such a small value, close to the lower limit previously reported [11–14] for LDHs containing intercalated chromate (8.13–10 Å), can be the result of a strong interaction between the chromate oxide anions and the brucite-like layers.

Table 1
Element chemical analyses (% weight), formulae and crystallographic parameters (Å) of synthesized chromate LDHs

Sample	Mg	Zn	Al	Cr	C	Formula	$d_{(003)}$	a	c
MgCCr	18.3		10.1	6.5	0.8	$[Mg_{0.67}Al_{0.33}(OH)_2](CrO_4)_{0.11}(CO_3)_{0.06}\ nH_2O$	8.57	3.04	25.7
MgNCr	19.96		10.2	7.0	0.5	$[Mg_{0.68}Al_{0.32}(OH)_2](CrO_4)_{0.11}(CO_3)_{0.04}\ nH_2O$	8.00	3.04	24.0
MgClCr	18.12		9.83	7.9	0.8	$[Mg_{0.67}Al_{0.33}(OH)_2](CrO_4)_{0.14}(CO_3)_{0.01}\ nH_2O$	8.66	3.04	26.0
ZnClCr		32.12	7.59	4.9	0.8	$[Zn_{0.67}Al_{0.33}(OH)_2](CrO_4)_{0.12}(CO_3)_{0.05}\ nH_2O$	8.54	3.07	25.62

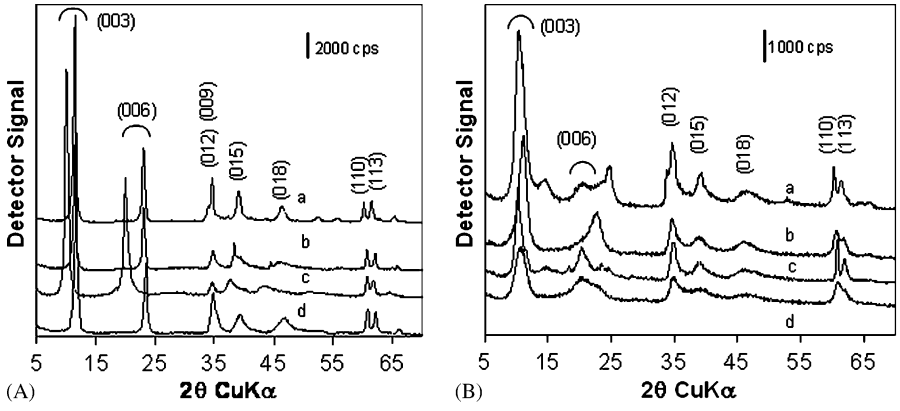

Fig. 1. PXRD patterns of (A) precursors samples (a) ZnAlCl (b) MgAlCl (c) MgAlN and (d) MgAlC, and (B) samples (a) ZnClCr (b) MgNCr (c) MgClCr and (d) MgCCr.

As expected, the values for crystallographic parameter *a*, Table 1, is the same for the samples with the same layer cations, while the values for parameter *c* are rather close to each other, as all samples should contain intercalated chromate. However, it should be noted that some of the (003) maxima are clearly asymmetric or rather broad; actually, those for samples MgClCr and ZnClCr clearly show a shoulder close to 7.7 Å, which could be ascribed to the presence of a by-product consisting of the corresponding chloride-LDH—as a result of incomplete exchange—or to contamination by a carbonate-LDH, as the spacings reported [30] for carbonate and chloride LDHs are very close to each other. However, from the element chemical analyses results, we should conclude the presence of the carbonate-LDH. In samples MgCCr and MgNCr containing carbonate the peaks do not split, but they are very broad, especially for sample MgCCr; probably the lines corresponding to the carbonate-containing LDH are obscured by the bands due to the chromate-containing one.

Calcination at increasing temperature (100–800 °C) gives rise to X-ray diffraction diagrams included in Figs. 2 and 3. In the MgAl–CrO_4 LDHs the maxima originated by the hydrotalcite-like phase persist (although they shift from their original positions) up to 300 °C, but disappear when the samples are calcined at 400 °C or above, indicating the appreciable stability attained upon intercalation of chromate.

As mentioned, as the temperature is raised from r.t. to 300 °C, in addition to an increase in the intensity of the (003) diffraction peak, there is also a shift towards larger 2θ values: the (003) diffraction peak is recorded at 8.66, 8.03, and 6.88 Å for the original sample MgClCr and after calcination at 150 and 300 °C, respectively. A similar behaviour is observed for samples MgNCr and MgCCr, for which the decrease in $d_{(003)}$ is from 8.0 to 6.9 Å and from 8.57 to 7.1 Å, respectively, from the unheated to the sample calcined at 300 °C.

The decrease in the gallery height is also observed for sample ZnClCr, Fig. 2B, the basal spacing decreasing from 8.54 to 7.47 Å when the sample is calcined at 200 °C. However, in this case, the structure collapses when the sample is calcined at 300 °C and the layered system is destroyed. This lower stability of sample ZnClCr, if compared to that of the samples containing Mg and Al in the layers (whichever the specific precursor used to prepare them) might be related to the fact that ZnO crystallises at a lower temperature than MgO does (the diffraction maxima corresponding to these two oxides can be clearly detected for the high-temperature calcined solids).

As mentioned above, the shrinkage of the gallery, decreasing the gallery height, when the oxometalate-containing LDHs are calcined at moderate temperatures, has been previously reported by different authors [11–13,22,31,32] and has been ascribed to a grafting process, i.e., anchoring of the oxometalates to the layers. Alternatively, such a decrease in the gallery height has been also claimed to occur as a consequence of dehydration of the samples at these moderate temperatures. In order to determine which of the two processes is responsible for the decrease of the gallery height of our samples, we have stored the samples, previously calcined at 200 °C, for 24 h

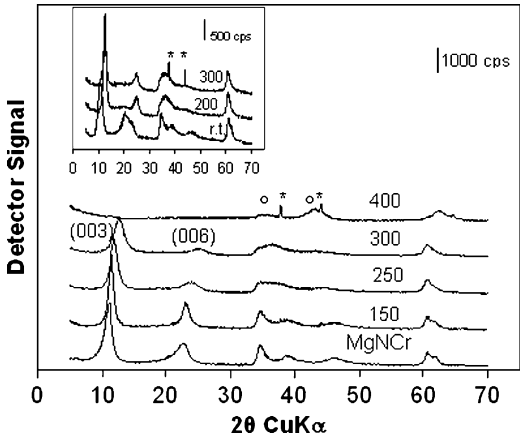

Fig. 3. PXRD patterns of samples MgNCr and MgCCr (inset), uncalcined and calcined at the temperatures given (°C). (*) Diffraction by the Al sample holder; (○) MgO.

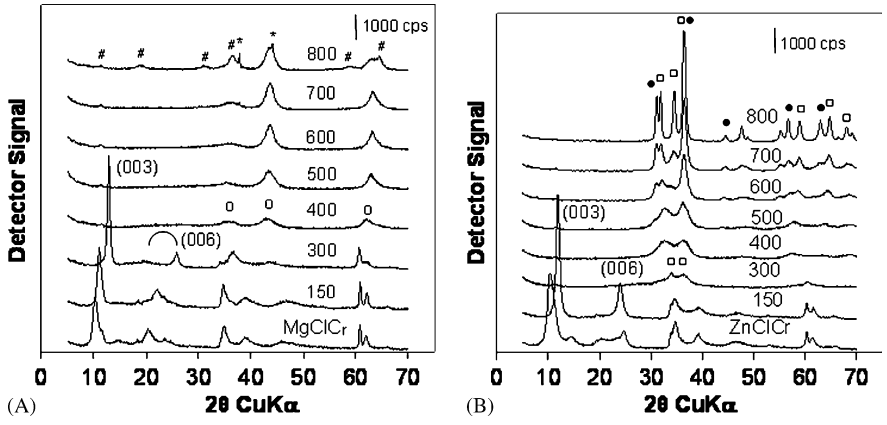

Fig. 2. PXRD patterns of samples (A) MgClCr and (B) ZnClCr, uncalcined and calcined at temperatures given (°C). (*) Diffraction by the Al sample holder; (○) MgO; (#) $MgAl_{1.5}Cr_{0.5}O_4$ spinel; (□) ZnO; (●) $ZnAl_2O_4$ spinel.

at r.t. in a desiccator, at saturation pressure of water vapour; the PXRD diagram has then been recorded and we have found that the spacing for the (003) reflexion is the same as for the sample calcined at 200 °C, i.e., this treatment is unable to expand the layers, demonstrating that the oxometalate is anchored to the layer [33]. This process has been explained assuming that one hydroxyl anion of the brucite-like layer is replaced by an oxide anion of the oxometalate, whose results definitively bonded to the layers.

Changes observed in the PXRD diagrams of the samples containing Mg and Al when they are heated above 300 °C is similar for all of them, Figs. 2 and 3. The layered structure is destroyed at 400 °C, and only weak, broad maxima are recorded at 2.43, 2.11, and 1.49 Å, which correspond to planes (111), (200), and (220) of MgO periclase, respectively (JCPDS file 4-0829 [34]). The sharpness of these peaks increases as the calcination temperature increases. When calcination is carried out at 800 °C, additional weak diffraction maxima are recorded, whose positions coincide with those for $MgAl_{1.5}Cr_{0.5}O_4$, a mixed oxide with the spinel structure, whose formation has also been reported upon calcination of MgCr-CO_3 and MgAl-(trisoxalochromate(III)) LDHs [35,36].

Calcination of sample ZnClCr at 300 °C, Fig. 2B, produces an almost amorphous phase, where only extremely weak peaks at 2.62 and 2.46 Å, ascribed to ZnO (JCPDS file 36-1451 [34]), are recorded; their intensities increase as the calcination temperature is increased. Additional to these signals, others due to $ZnAl_2O_4$ spinel (JCPDS file 5-0009 [34]) are also recorded from 600 °C and above, and their intensities also increase with the calcination temperature. No diffraction line ascribable to chromium-containing solids was recorded for these samples, so we should conclude that chromium-containing species should be well dispersed in this system.

Representative FT-IR spectra of the samples have been included in Fig. 4. The broad band at 3462-3445 cm^{-1} is due to the stretching mode of hydroxyl groups, both from the layers and of interlayer water molecules; in addition, these are also responsible for the medium–weak intensity band at 1630 cm^{-1}, due to their bending mode. The bands recorded in the low wavenumbers region are due to Al/Mg-OH or Zn/Al-OH translational modes of layer hydroxyl groups, recorded at 552, 448, and 390 cm^{-1} for the Mg,Al samples and at 552, 427, and 324 cm^{-1} for the ZnClCr sample [37,38]. The v_3 mode of intercalated carbonate is recorded in all samples at 1360 ± 8 cm^{-1}. The characteristic infrared band of chromate, due to mode v_d(Cr–O), recorded at 890 cm^{-1} for free chromate [39], is recorded at 883, 884, 877, and 870 cm^{-1}, respectively, for samples MgCCr, MgNCr, MgClCr, and ZnClCr. The shift observed (up to 20 cm^{-1} in some cases) indicates that the Cr–O bond is weaker than for free chromate, probably through hydrogen bonding of the anion with interlayer water molecules of layer hydroxyl groups.

When MgAl–CrO_4 LDHs are calcined, the spectra recorded are essentially the same, whichever the precursor used. In all cases, the band due to mode v_d(Cr–O) of chromate splits, even after calcination at 100 °C, from the initial position at ca. 880 cm^{-1}, into two bands at 880 and 940 cm^{-1} for the samples prepared by reconstruction, and at 864 and 930 cm^{-1} for sample MgClCr. In the meanwhile, some minor changes in the low wavenumbers region, where bands due to the modes within the layers are recorded, are also observed. These changes are also observed when sample ZnClCr is calcined, Fig. 4B, and the bands at 864 and 930 cm^{-1} are observed when the calcination temperature is 100–200 °C. All these changes further confirm that oxometalate is grafted on calcination at moderate temperatures, with a decrease in the symmetry of the chromate anion from T_d to C_{3v} or even C_{2v}, as a consequence of its interaction with the brucite-like layers [14,40] by a OH(brucite)/O(oxometalate) substitution.

On the other hand, the FT-IR spectra recorded for MgAl–CrO_4 LDHs calcined below the temperature needed to destroy the layered structure, show a splitting of the v_3 mode of carbonate at 1384 and 1350 cm^{-1}, and a new band at 1543 cm^{-1} develops. Bands in these same ranges have been previously reported by other authors, who claim they

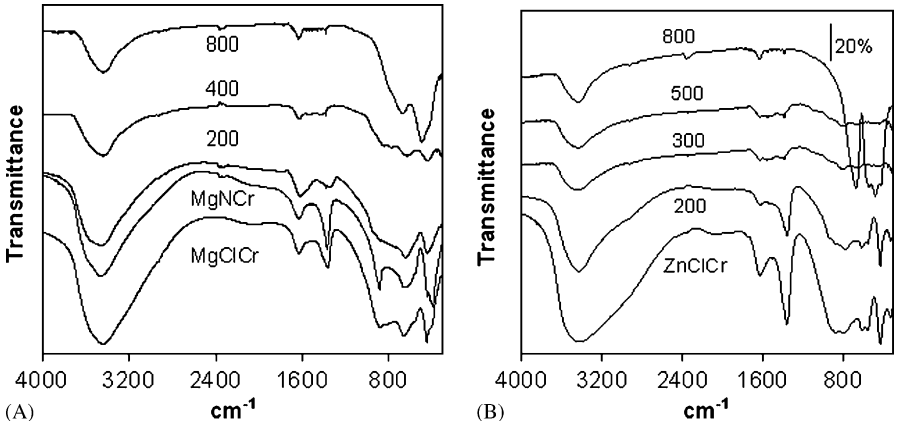

Fig. 4. FT-IR spectra of samples (A) MgNCr and uncalcined and calcined MgClCr and (B) uncalcined and calcined ZnClCr; calcination was performed at the temperatures given (°C).

are due to the presence of hydrogencarbonate species, formed via dehydration of the carbonate-LDH, by transferring a proton from the layer hydroxyls to the interlayer carbonate anion [37,41].

Calcination of MgAl–CrO_4 LDHs samples at 400 °C (when the layered structure is destroyed, according to the PXRD data) gives rise to FT-IR spectra, Fig. 4A, with very weak absorption bands whose positions coincide with those of the bands recorded for the sample calcined at 300 °C (940, 864, 611, 552, 428, and 324 cm^{-1}), indicating that, despite the information provided by the XRD experiments, a fraction of mostly amorphous MgAl–CrO_4 LDH still exists. The layered structure, however, is completely destroyed at 500 °C, when crystallisation of MgO begins; these changes give rise to the developing of two new bands, at 671 and 476 cm^{-1}, whose intensity is enhanced and the second one shifts to 492 cm^{-1} when calcination is carried out at 700 and 800 °C, probably due to an increase in the crystallinity of MgO. It should be noticed that no band due to mode ν(Cr–O) of $MgAl_{1.5}Cr_{0.5}O_4$ is recorded, even in samples calcined at 800 °C, the temperature at which that species was detected by XRD, probably because they are masked in the much broader and intense bands due to MgO.

The FT-IR spectrum recorded for sample ZnClCr calcined at 300 °C is characteristic of an amorphous phase, and none of the bands detected at low temperature is recorded. According to the PXRD data, the layered structure is destroyed at 300 °C. Bands at 672 and 504 cm^{-1}, characteristic of ZnO, develop after calcination at 500 °C and when calcination is carried out between 600 and 700 °C additional bands at 554, 481, and 421 cm^{-1}, probably due to $ZnAl_2O_4$ spinel already detected by XRD, are recorded. These bands become stronger and sharper when the calcination temperature is increased. Samples ZnAl-Cl and ZnAl-CO_3 give rise to similar spectra when they are calcined between 300 and 800 °C; so, FT-IR spectroscopy is unable to evidence the presence of crystalline Zn–Al–Cr–O phases in this temperature range.

It is well known [42] that the strong yellow colour of chromate species is due to a charge transfer process $O^{2-} \rightarrow Cr^{6+}$ recorded in the visible range of the electromagnetic spectrum, as *d–d* transitions are impossible because of the d^0 configuration of chromium in chromate. The vis–UV spectrum of solid K_2CrO_4, recorded following the diffuse reflectance technique, shows absorption bands at 459, 340, 265, and 229 nm. These bands shift to 440, 372, and 275 nm when chromate is in aqueous solution. The vis–UV/DR spectra of original and calcined MgClCr and ZnClCr samples are included in Fig. 5. The bands recorded in the spectra of sample MgClCr calcined up to 500 °C are very similar (they are recorded at 445, 370, 358, and 270 ± 2 nm), and essentially coincide with those of the chromate anion. Calcination at 500 °C gives rise to an additional, weaker, band at 604 nm, and still a new band at 706 nm is recorded for the sample calcined at 800 °C. The first bands further confirm the presence of chromate in all MgAl LDHs, even

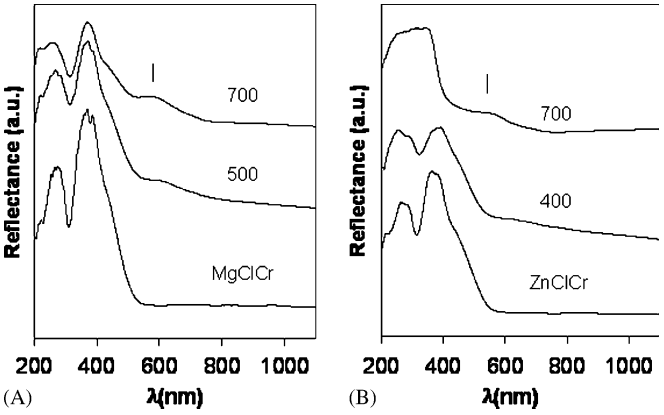

Fig. 5. Vis–UV/DR spectra of samples (A) MgClCr and (B) ZnClCr, uncalcined and calcined at the temperatures given (°C).

at rather high temperature. The last bands mentioned can be ascribed to the Laporte forbidden transition since the fundamental state $^4A_{2g}(F)$ to the excited state $^4T_{2g}(F)$ (the band at 604 nm) and to a spin-forbidden transition (band at 706 nm) [43] of Cr^{3+} in octahedral coordination. The last band is known as the ''ruby band'' [44]. The other bands originated by octahedrally coordinated Cr^{3+} species due to transitions $^4A_{2g}(F) \rightarrow {}^4T_{1g}(P)$ and $^4A_{2g}(F) \rightarrow {}^4T_{1g}(F)$, which are usually recorded at 420 and 270 nm, are probably masked by the intense bands originated by the chromate species.

Formation of Cr^{3+} after calcination is also evidenced by the green colour that the original yellow samples adopt as the calcination process is carried out, as they are progressively calcined. After combination with MgO and Al^{3+} species, the compound $MgAl_{1.5}Cr_{0.5}O_4$ is formed; its presence has been proved by PXRD analysis at high temperature (800 °C).

The vis–UV/DR spectra recorded for sample ZnClCr calcined up to 300 °C, Fig. 5B, are similar to those shown by the MgAl-CrO_4 LDHs uncalcined or calcined up to 400 °C; only the intense charge transfer bands due to tetrahedrally coordinated oxo-Cr^{6+} species are recorded (at 448, 388, 363 and 285 nm). However, at 400 °C (at this temperature the samples show a greenish colour) and above the spectrum includes also a very weak band at 605 nm, characteristic of octahedrally coordinated Cr^{3+} species. The colour becomes finally grey when the sample is calcined at 700 °C, and the spectrum shows (Fig. 5B) a broad band from 240 to 344 nm, similar to that recorded in the spectrum of ZnO, a species whose presence had been confirmed by PXRD and FT-IR spectroscopy. Other bands recorded at 561 and 671 nm are due to Cr^{3+} species, probably dispersed in the lattice of ZnO formed during calcination.

Changes in the average oxidation state of chromium in the samples prepared, and submitted to calcination at different temperatures have been monitored by TPR. The TPR profiles for samples MgClCr and ZnClCr are included in Figs. 6A and B, respectively. We have previously

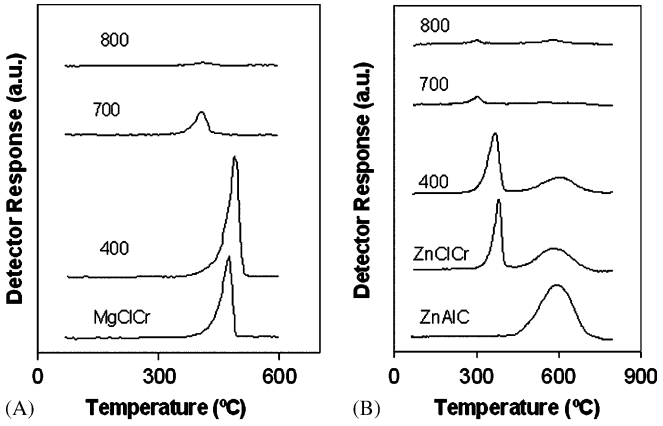

Fig. 6. TPR profiles of samples: (A) uncalcined and calcined MgClCr, and (B) uncalcined ZnAlC and uncalcined and calcined ZnClCr; calcination was performed at the temperatures given (°C).

reported [45] that under the experimental conditions here used Mg^{2+}, Al^{3+}, or CO_3^{2-} species are not reduced. However, we have checked reducibility of ZnAl-CO_3 LDH (sample ZnAlC), whose TPR profile shows a reduction maximum centred at 600 °C, Fig. 6B, which should be due to reduction of Zn^{2+} to Zn^0, of ZnO formed during heating of the sample in the TPR analysis. It should be noticed that the reduction processes detected by TPR cannot be ascribed to reduction of the species as they were in the original, non-heated LDH, as its structure changes during the heating TPR process. Although commercial ZnO does not show any reduction peak in its TPR profile, it is well known that ZnO develops lattice defects when heated in vacuo or under reducing conditions, leading to the formation of non-stoichiometric compounds usually formulated as $Zn_{1+x}O$ [46], which destabilise the lattice and thus further facilitate zinc reduction. As already reported in this study, sample ZnClCr, as the ZnAlC one, decomposes upon heating producing ZnO, which, at moderate calcination temperatures, should contain an appreciable concentration of lattice defects, thus favouring Zn^{2+} reduction. This reduction effect is recorded for the original and calcined ZnClCr samples, together with another reduction maximum whose position shifts from 371 to 285 °C, Table 2, when the precalcination temperature increases, and which corresponds to reduction of Cr^{6+} to Cr^{3+}.

The TPR curves for the original and calcined MgClCr samples shows, Fig. 6A, only one maximum due to reduction from Cr^{6+} to Cr^{3+}, whose precise positions are included in Table 2. The position of the maximum reduction peak, as in the Zn-containing samples occurs, shifts to lower temperatures (from 480 to 405 °C) as the precalcination temperature increases, and when the sample is precalcined above 400 °C, the intensity of this peak strongly decreases (it is even hardly detected when the sample has been precalcined at 800 °C).

Hydrogen consumption has been determined from the areas under the peaks, after calibration with commercial (from Merck) CuO, assuming the following reactions to take place (previous results [45] have shown that Cr^{3+} species are not reduced under the experimental conditions here used):

$$Cr^{6+} + 3H_2 \rightarrow Cr^{3+} + 6H^+,$$
$$Zn^{2+} + H_2 \rightarrow Zn^0 + 2H^+.$$

Table 2
TPR data, temperature of the reduction maxima, molar ratio and Cr(VI) and Zn(II) reduction percentages

Sample	T_{Max}(°C)	H_2/Cr^a	H_2/Zn^a	% Cr^{6+}	% Zn^{2+}
ZnAlC	600		0.6		30
ZnClCr	588, 371	1.2	0.46	40	23
ZnClCr/400	605, 357	2.0	0.34	67	17
ZnClCr/700	552, 285	0.2	0.04	6	2
ZnClCr/800	582, 285	0.06	0.04	2	2
MgClCr	471	0.9		30	
MgClCr/400	480	1.5		50	
MgClCr/700	397	0.24		8	
MgClCr/800	400	0.07		3.6	

[a]Molar ratio.

The calculated reduction percentages have been included in Table 2 for both cations, Cr^{6+} and Zn^{2+}. The percentage of reduction from Cr^{6+} to Cr^{3+} for samples MgClCr and ZnClCr (as well as for those prepared by reconstruction, MgNCr and MgCCr) increases as the precalcination temperature increases, the largest value being measured for the samples precalcined at 400 °C. This indicates that reduction of interlayer chromate is more difficult than when existing in the amorphous phase formed by collapsing of the layered structure. Above 400 °C the reduction percentage strongly decreases, reduction being almost unobservable in samples precalcined at 800 °C. This decrease is a consequence of the partial reduction of Cr^{6+} to Cr^{3+} during precalcination of the samples above 400 °C (as concluded from vis–UV spectroscopic studies).

In agreement with previous results [36,45,47] in no case could the reduction observed be ascribed to reduction to zero-valent chromium.

The FT-IR spectra recorded after r.t. adsorption of pyridine and outgassing at increasing temperatures on MgAl–CrO_4 and ZnAl–CrO_4 LDHs calcined at 300 or 400 °C are almost coincident in both cases; for simplicity, the spectra included in Fig. 7 are those corresponding to sample MgClCr calcined at 400 °C. Bands at 1609, 1589, 1575, 1489, and 1443 cm^{-1} are observed in all these spectra; they are due to modes 8*a*, 8*b*, 19*a*, and 19*b* of pyridine adsorbed on surface Lewis acid sites [48,49]. The weakness of the bands, as well as the fact that they disappear by simply outgassing the samples at 200 °C, indicates that the surface sites are weak Lewis acid sites; it also seems (although true quantification cannot be concluded from the results so far obtained) that the Zn-containing sample should possess a lower surface acidity, as the bands

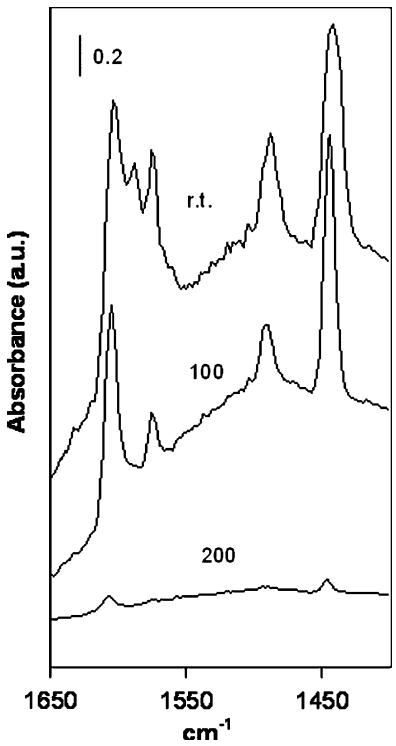

Fig. 7. FT-IR spectra of py adsorption at room temperature and after outgassing at temperatures given (°C) on sample MgClCr calcined at 400 °C.

recorded for this sample are weaker than those recorded for the Mg-containing samples. Splitting of the band due to mode 8*a* (the bands are recorded at 1605 and 1589 cm^{-1}) indicates the simultaneous presence, on the surface of the samples, of two types of surface acid Lewis sites, probably associated to surface coordinatively unsaturated Cr^{6+} and Mg^{2+} (or Zn^{2+} in samples containing Zn) cations. The surface Lewis sites associated to surface Mg^{2+}(or Zn^{2+}) cations should also be weaker than the other ones, as the band at 1589 cm^{-1} disappears upon outgassing at 100 °C. Although the presence of surface Brönsted acid sites has been reported for Cr^{6+}/TiO_2 systems [50], they have not been detected in our samples, probably due to the large basicity of the existing oxide anions.

Pyridine adsorption on samples calcined above 400 °C gives rise to FT-IR spectra with bands that quickly disappear after outgassing at r.t., which indicates that only physisorption of pyridine took place. The absence of surface Lewis acid sites is due to reduction from Cr^{6+} to Cr^{3+} upon heating above 400 °C, as detected by vis–UV spectroscopy and TPR.

The nitrogen adsorption–desorption isotherms, recorded at −196 °C for all chromate-containing LDHs show features which can be ascribed to types I and II in the IUPAC classification [51]. This can be related to the presence of microporous or non-porous materials. The values for the specific surface areas, determined following the BET method [51], are included in Table 3, and they increase when the calcination temperature is increased.

Table 3
Specific surface area ($m^2 g^{-1}$) and pore volume of the samples

Sample	S_{BET}	S_t	S_M	V_p ($cm^3 g^{-1}$)
MgClCr	36	20	15	0.09
MgClCr/400	56	47	8	0.10
MgClCr/700	124	n.d.	n.d.	n.d.
MgClCr/800	15	n.d.	n.d.	n.d.
ZnClCr	32	26	5	0.12
ZnClCr/400	51	45	6	0.14
ZnClCr/700	37	n.d.	n.d.	n.d.
ZnClCr/800	35	n.d.	n.d.	n.d.

n.d., not determined.

The highest specific surface areas for samples containing Mg and Al are reached when the samples are calcined up to 700 °C; so, although the values for the uncalcined samples MgCCr, MgNCr, and MgClCr are 15, 14, and 36 $m^2 g^{-1}$, respectively, they increase up to 45, 67, and 124 $m^2 g^{-1}$ when calcined at 700 °C. When the calcination temperature is 800 °C, the specific surface area values decrease. Such a decrease is observed for sample ZnClCr from 600 °C upwards.

These changes in the specific surface areas can be related to the nature of the crystallographic species existing in these samples, as they cannot be related to formation of channels and pores upon removal of the interlayer anion, as proposed elsewhere [52] when the interlayer anion is carbonate or nitrate. Such a specific surface area development could also be related to the presence of small contaminating amounts of interlayer carbonate or chloride, which are expelled from the solid on calcination as CO_2, Cl_2 or HCl, thus giving rise to enhanced porosity and thus surface area development [52]; however, the larger surface area enhancement is observed for those samples where contamination by these species is lower. So, we should conclude that the increase in the specific surface area should be mostly related to formation of amorphous species, such as $MgAl_{1.5}Cr_{1.5}O_4$, dispersed in the MgO lattice, which crystallise only at 800 °C, as shown by the PXRD diagrams. In a similar way, both Cr^{3+} and Cr^{6+} species exist in sample ZnClCr, well dispersed in the ZnO matrix up to 500 °C, and the Zn, Al spinel crystallise between 600 and 700 °C, the same temperature range where a decrease in the specific surface area is observed.

Finally, the *t*-plots for all samples show a positive zero-intercept, indicating the presence of micropores. The values for the external surface areas, S_t [53] and area equivalent to adsorption in micropores, S_M, are included in Table 3. The area equivalent to adsorption in micropores decreases when the calcination temperature is increased; it is well known [5,10] that LDHs with small interlayer anions (i.e., chloride, nitrate, carbonate) do not show microporosity; however, on intercalating bulk anions, such as chromate, accesible voids and pores develop, which are easily accessible to nitrogen molecules, thus accounting for the microporosity here found.

4. Conclusions

Both synthesis methods used here, anion exchange and reconstruction, lead to formation of acceptably crystalline LDHs containing intercalated chromate, with basal spacings ranging from 8 to 8.6 Å, which decrease when the samples are calcined; this decrease is a consequence of a grafting process arising from a strong interaction between the oxometalate and the hydroxyl layers.

Synthesis of these systems by reconstruction from LDHs containing intercalated nitrate calcined at moderate temperatures is reported here for the first time; it seems to be a better way than reconstruction from calcined carbonate precursors, as better crystallised samples are prepared in a faster way, without an excessive decrease of the pH of the suspension.

The MgAl–CrO_4 LDHs prepared are more stable (up to 400 °C) than the ZnAl analogues (300 °C) due to a fast formation of crystalline ZnO in the last case; actually, only ZnO is detected by PXRD after collapsing of the layered structure up to 600 °C where crystallisation of a Zn,Al spinel starts. Destruction of the hydrotalcite-like structure in MgAl–CrO_4 systems around 400 °C takes place with simultaneous formation of mostly amorphous MgO, whose crystallinity increases as the calcination temperature is increased. A new spinel phase, with a composition $MgAl_{1.5}Cr_{0.5}O_4$, is formed at 800 °C.

Cr(VI) species are more easily reduced to Cr(III) species in the ZnClCr systems than in MgAl–CrO_4 ones, as it takes place at a lower temperature and in a larger percentage. All systems calcined in the 300–400 °C range show Lewis surface acid sites. Reduction of Cr(VI) to Cr(III) takes place when the samples are calcined above 400 °C, cancelling the Lewis surface acid sites, whose presence has been detected in samples calcined below this temperature by FT-IR monitoring of pyridine adsorption; samples calcined above 400 °C are no longer reduced along the TPR experiments.

Acknowledgments

Authors thank financial support from MCyT (Grant MAT2003-06605-C02-01) and EFRD, and to Mr. A. Montero for his assistance in obtaining some of the experimental results; DC acknowledges a grant from Universidad de Salamanca.

References

[1] R. Allmann, Z. Kristalogr. 126 (1949) 417.
[2] Q. Norwacki, R. Schneidegger, Helv. Chim. Acta 36 (1952) 375.
[3] W. Feitnetch, G. Fischer, Helv. Chim. Acta 18 (1935) 555.
[4] W.T. Reichle, Solid State Ion 22 (1986) 135.
[5] F. Cavani, F. Trifiró, A. Vaccari, Catal. Today 11 (1991) 173.
[6] A. de Roy, C. Forano, K. El Malki, J.P. Besse, Synthesis of microporous materials, in: M.L. Ocelli, H.E. Robson (Eds.), Expanded Clays and Other Microporous Solids, vol. II, Van Nostrand Reinhold, New York, 1992, p. 108.
[7] S.P. Newman, W. Jones, New J. Chem. 22 (1998) 105.
[8] F. Kooli, I.C. Chisem, M. Vucelic, W. Jones, Chem. Mater. 8 (1996) 1969.
[9] S. Carlino, Solid State Ion 98 (1997) 73.
[10] V. Rives (Ed.), Layered Double Hydroxides: Present and Future, Nova Science Publishers, Inc., New York, 2001.
[11] K. Chibwe, W. Jones, J. Chem. Soc. Chem. Commun. 14 (1989) 926.
[12] F. Malherbe, J.P. Besse, J. Solid State Chem. 155 (2000) 332.
[13] F. Malherbe, L. Bigey, C. Forano, A. de Roy, J.P. Besse, J. Chem. Soc., Dalton Trans. (1999) 3831.
[14] C. Forano, A. De Roy, C. Depége, M. Khaldi, F.Z. Métoui, J.P. Besse, Synthesis of porous materials, in: M.L. Ocelli, H. Kessler (Eds.), Zeolites, Clays and Nanostructures, Marcel Dekker Inc., New York, 1996, p. 675.
[15] B. Houri, A. Legrouri, A. Barrong, C. Forano, J.P. Besse, Collect. Czech. Chem. Commun. 63 (1998) 732.
[16] B. Houri, A. Legrouri, A. Barrong, C. Forano, J.P. Besse, J. Chim. Phys. 96 (1999) 455.
[17] N.K. Lazaridis, K.A. Matis, M. Webb., Chemosphere 42 (2001) 373.
[18] N.K. Lazaridis, A. Hourzemanoglou, K.A. Matis, Chemosphere 47 (2002) 319.
[19] R.L. Goswamee, P. Senupta, K.G. Bhattacharyya, D.K. Dutta, Appl. Clay Sci. 13 (1998) 21.
[20] W.T. Reichle, J. Catal. 63 (1980) 295.
[21] M. del Arco, S. Gutiérrez, C. Martín, V. Rives, J. Rocha, J. Solid State Chem. 151 (2000) 272.
[22] K. El Malki, A. De Roy, J.P. Besse, Eur. J. Solid State Inorg. Chem. 26 (1989) 339.
[23] F. Burriel, F. Lucena, S. Arribas, J. Hernández, Química Analítica Cuantitativa, Paraninfo, Madrid, 1989.
[24] P. Malet, A. Caballero, J. Chem. Soc. Faraday Trans. I 84 (1988) 236.
[25] V. Rives, C. Martín, A. Montero, Spanish Patent, 200100688, 2001.
[26] P. Gay, The Crystalline State. An Introduction,, Oliver & Boy, Edinburgh, 1972.
[27] M. Belloto, B. Rebours, O. Clause, J. Linch, D. Bazim, E. El Kaïm, J. Phys. Chem. 100 (1996) 8527.
[28] M.A. Drezdzon, Inorg. Chem. 27 (1988) 4628.
[29] T.C. Waddington, Adv. Inorg. Chem. 1 (1959) 180.
[30] A. Roy, C. Forano, J.P. Besse, in: V. Rives (Ed.), Layered Double Hydroxides: Present and Future, Nova Science Publishing Co. Inc., New York, 2001, p. 1 (Chapter 1).
[31] M. del Arco, D. Carriazo, S. Gutiérrez, C. Martín, V. Rives, Inorg. Chem. 43 (2004) 375.
[32] V.R.L. Constantino, T.J. Pinnavaia, Inorg. Chem. 34 (1995) 883.
[33] X. Hou, D.L. Bish, S.L. Wang, C. Johnston, R. Kirkpatrick, J. Am. Miner. (2003) 88.
[34] JCPDS: Joint Committee on Powder Diffraction Standars, International Centre for Diffraction Data, Pennsylvania (USA), 1977.
[35] M. del Arco, M.V.G. Galiano, V. Rives, R. Trujillano, Inorg. Chem. 33 (1996) 6362.
[36] M. del Arco, S. Gutiérrez, C. Martín, V. Rives, Inorg. Chem. 42 (2003) 4232.
[37] J.T. Kloprogge, R.L. Frost, in: V. Rives (Ed.), Layered Double Hydroxides: Present and Future, Nova Science Publishing Co. Inc., New York, 2001, p. 139 (Chapter. 5).
[38] J.T. Kloprogge, in: J.T. Kloprogge (Ed.), The application of vibrational spectroscopy to clay minerals and layered double hydroxides, CMS Workshop Lectures, vol. 13, The Clay Mineral Society, Aurora, CO, 2005, p. 203.
[39] K. Nakamoto, Infrared and Raman of Inorganic and Coordination Compounds, Wiley, New York, 1986.
[40] D. Loüer, M. Loüer, D. Guandjean, Acta Crystallogr. B 29 (1973) 1696.
[41] A. Vaccari, L. Zatorski, Appl. Catal. 73 (1991) 217.
[42] K. Fuda, K. Suda, T. Matsunaga, Chem. Lett. (1993) 1479.
[43] A.B.P. Lever, Inorganic Electronic Spectroscopy, Elsevier, Amsterdam, 1984.
[44] S.S. Eaton, T.D. Yager, G.R.J. Eaton, Chem. Educ. 56 (1979) 635.

[45] V. Rives, M.A. Ulibarri, A. Montero, Appl. Clay Sci. 10 (1995) 83.
[46] R.J. Tilley, Deffect Crystal Chemistry and its Applications, Blakie, London, 1987.
[47] M. del Arco, V. Rives, R. Trujillano, P. Malet, J. Mater. Chem. 6 (1996) 1419.
[48] E.P. Parry, J. Catal. 2 (1963) 371.
[49] E.B. Wilson, Phys. Rev. 45 (1934) 706.
[50] A.M. Venezia, L. Palmisano, M. Schiavello, C. Martín, V. Rives, J. Catal. 147 (1994) 115.
[51] K.S.W. Sing, D.H. Everett, R.A.W. Hall, L. Moscou, L. Pierotti, J. Rouquerol, T. Sieminiewska, Pure Appl. Chem. 57 (1985) 603.
[52] W. Kagunya, W. Jones, Appl. Clay Sci. 10 (1995) 95.
[53] B.C. Lippens, J.H. de Boer, J. Catal. 9 (1957) 143.